Coupling Tracking and Control in the Dynamic Wireless Charging for Electric Vehicles

Chen Kaiwen[1] Luo Junyuan[2] Ouyang Yuzhao[2] Jia Yipeng[2] J. F. Pan[2] Eric Ka-Wai Cheng[1]
[1] Power Electronics Research Center, Dept. of Electrical Engineering, The Hong Kong Polytechnic University, Hong Kong;
[2] College of Mechatronics and Control Engineering Shenzhen University Shenzhen, China
E-mail: kris-kaiwen.chen@connect.polyu.hk

Abstract: In the wireless charging for the moving electric vehicles (EVs), the unstable coupling that largely influences the output robustness is brought by the dynamic manner. In this paper, a control scheme based on a simple LC compensated dynamic wireless charging couplers is proposed, where the exact mutual inductance is extracted by monitoring the direct current (dc) current and voltage outputs. The maximum total efficiency is thus achieved by adjusting the voltage inputs for the transmitters (Txs). A 200mm*100mm Tx array is modeled, and the overlap area is 50% of the size in the simulation and experiment. The performance of the control strategy is proved by the experimental results, and the efficiency could be universally improved by 2.1%~5.2%.

Keywords: wireless charging; mutual inductance extraction, maximum efficiency, control strategy

I. INTRODUCTION

Dynamic wireless charging allows the electric vehicles freely move on the transmitter array while there is little interruption to power transfer [1-2]. However, the power output is frequently disturbing due to the coupling between the Txs and Rx is varying with car movement.

The goals of a well-established dynamic charging system are satisfied stability and maximum total efficiency. The maximum energy efficiency transfer (MEET) is achieved by finding the optimized ratio of primary currents in Txs [3]. The currents of each Tx coil are synchronously adjusted so that the reflected impedance of Rx is the optimized load impedance.

The MEET has been established for multi-Tx charging system by many research forces, and the requirements could be concluded as following:
a) The ratio of the primary currents should be found by I_{P1}:I_{P2}:I_{P3}:...:I_{Pn}=M_{1S}:M_{2S}:M_{3S}:...:M_{nS}, where the M_{nS} is the mutual inductance between Tx_n and Rx
b) The speed of tracking must be fast enough to calibrate the mutual inductance and the real-time control output

There are many methods to perform MEET in different environments. The most simple and robust way is the perturb and observe (P&O). The variation of the mutual inductance is not necessarily found in this method, however, the real-time output voltage and current are sensed to calculate the system efficiency. The secondary side of wireless power transfer (WPT) system is linked to a dc/dc buck-boost converter, which is applied for adjusting the load impedance [4-5]. However, the P&O method relies badly on the iteration process, where the optimum load is usually converged after seconds delay [6].

Linear control algorithms are thus proposed to overcome the delay. The better run time performance is realized by integrating proportion integral (PI) control [7]. The error between reference maximum voltage gain and real value is detected as the input of PI controller. The limitation of linear control is that the error cannot be found in LCC resonant inverter due to its constant current property [8].

A straight way of tracking the maximum power efficiency is to find the exact mutual inductance. By sensing the impedance and voltage, it is possible to extract coupling coefficient precisely [9-10]. In the control strategy introduced in [11], the first step is to reveal the initial mutual inductance, and the second step is to estimate the latest coupling. This method is rather simple because the resonant current is not measured, nevertheless, it still has large delay of a few hundred milliseconds.

Based on the reviewof aforementioned references, few of them are developed based on a multiple Txs system, which is the practical model of dynamic charging. In addition, the control delays of some methods is too large to be used in charging EVs. To achieve better real time performance, a control scheme based on the extracted mutual inductance is proposed in this paper, where only dc real time values are needed. The relation between the optimum load impedance and the input voltage of each Tx is established. In section II, a 3 Txs and 1 Rx (3-to-1) charging system is modeled, which is regarded as the vehicle motion when drive over the power array. Then, the mutual inductance ratio and exact values are calculated under certain proper assumption. The control scheme is proposed in section III, where the optimum voltage is derived. In section IV, the simulation and experiments are proceed so that the stability of the output and total efficiency are proved to be improved.

II. MODELLING AND CONTROL STRATEGY

2.1 System model
The dynamic charging system consists of DC voltage inputs, bridge inverters, Tx array and a receiver. In this paper, the 3 Txs and 1 Rx (3-to-1) model is adopted in all analysis.

The basic construction is demonstrated in Fig.1. Besides the electronic components, the mutual inductance among Txs and Rx is marked. Differed from 1-to-1 charging, there are multiple couplings that could influence the behavior in the same time. Among them, M_{1S}, M_{2S} and M_{3S} significantly contribute to the transferred power and efficiency. Hence, for easy analysis, it can be assumed that the mutual inductance among Txs (M_{12}, M_{13}, M_{23}) is neglected. The weak coupling M_{kS} would bring lower efficiency, and thus the power input of this winding should be adjusted to a lower level so as to avoid producing exceeded reactive power. The voltage of the winding $U_{in,k}$ should be frequently controlled after its relation

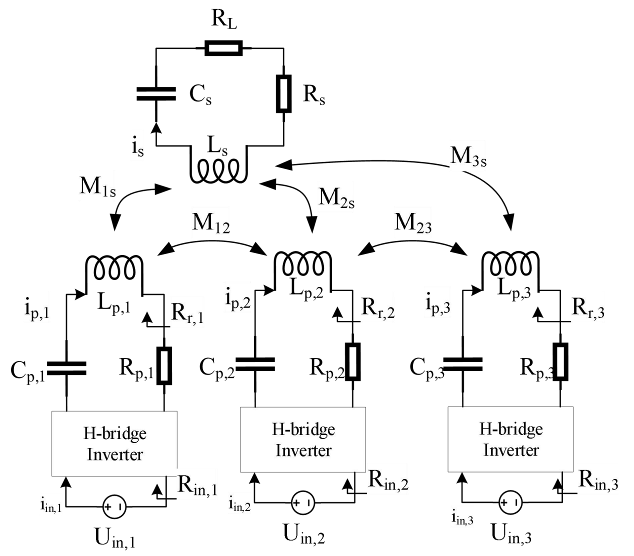

Fig. 1: System model of 3-to-1 dynamic wireless charging

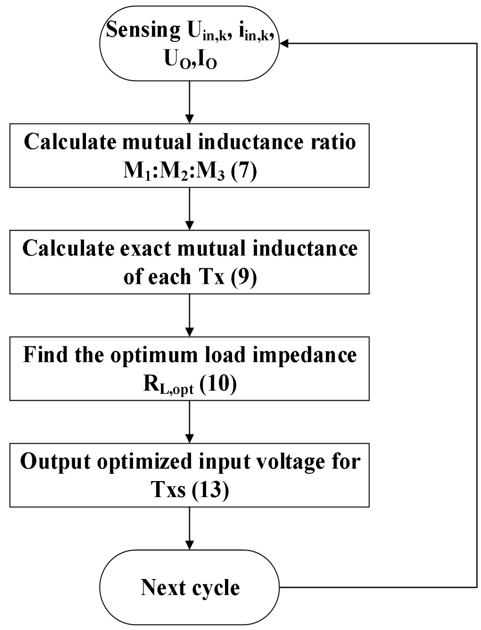

Fig.2: Control scheme flowchart

with mutual inductance is precisely found.

2.2 The extraction of mutual inductance ratio

Inheriting the equivalent circuit shown in Fig. 1, the ac voltage inputs and secondary side current can be calculated by Kirchhoff Voltage Law (KVL) in (1).

$$\begin{pmatrix} U_{in,a} \\ U_{in,b} \\ U_{in,3} \\ 0 \end{pmatrix} = \begin{pmatrix} Z_{P,1} & j\omega M_{12} & j\omega M_{13} & j\omega M_{1S} \\ j\omega M_{12} & Z_{P,2} & j\omega M_{23} & j\omega M_{2S} \\ j\omega M_{13} & j\omega M_{23} & Z_{P,3} & j\omega M_{3S} \\ j\omega M_{1S} & j\omega M_{2S} & j\omega M_{3S} & Z_{S}+R_L \end{pmatrix} \begin{pmatrix} i_{P,1} \\ i_{P,2} \\ i_{P,3} \\ i_S \end{pmatrix} \quad (1)$$

where

$$Z_{P,k} = \frac{1}{j\omega C_{P,k}} + j\omega L_{P,k} + R_{P,k} \quad (2)$$

$$Z_{S} = \frac{1}{j\omega C_{S}} + j\omega L_{S} + R_{S} \quad (3)$$

The reflected voltage, which is also the voltage of the Tx inductors, is

$$U_{r,k} = j\omega M_{kS} i_S \quad (4)$$

Hence, the reflected resistance can be calculated as following equation (5).

$$R_{r,k} = \frac{U_{r,k}}{i_{P,k}} j\omega M_{kS} i_S = j\omega M_{kS} \frac{i_S}{i_{P,k}} \quad (5)$$

The reflected resistance is an ac resistance and cannot be measured directly, but the relation with the input equivalent resistance could be found as (6).

$$R_{r,k} = \frac{\pi^2}{8} R_{in,k} - R_{P,k} \quad (6)$$

Consequently, the ratio of the mutual inductance could be expressed as the division of reflected resistance and the input voltage.

Table 1 Key parameters of the experiment setup

Parameter	Value	Parameter	Value
L_P	25μH	L_S	25μH
C_P	5.6μF	C_S	5.6μF
R_P	0.312Ω	R_S	0.325Ω
U_{in}	10V	R_L	5Ω

$$\frac{M_{aS}}{M_{bS}} = \frac{\left(\pi^2 R_{in,a}/8 - R_P\right) R_{in,b}}{\left(\pi^2 R_{in,b}/8 - R_P\right) R_{in,a}} \frac{U_{in,a}}{U_{in,b}} \quad (7)$$

The $i_{in,k}$ and $U_{in,k}$ can be easily obtained by the micro-controller, and the ratio can be calculated in dc observed values. The equation (7) is important because the ratio is not only used to indicate the input power, but also needed to acquire exact value of each mutual inductance.

2.3 Calculation of exact mutual inductance

The receiver output voltage UO is

$$U_O = \frac{\pi^2}{4} \frac{\omega R_L}{R_S + R_L} \sum_{n=1}^{3} (M_{nS} i_{P,n}) \quad (8)$$

Due to the primary current fulfill the assumption $I_{P1}:I_{P2}:I_{P3}:\ldots:I_{Pn} = M_{1S}:M_{2S}:M_{3S}:\ldots:M_{nS}$, the exact mutual inductance M_{kS} is written as

$$M_{kS} = \frac{4U_O\left(R_S + R_L\right)}{\pi^2 \omega R_L \left(\frac{1}{2} i_{in,k} + \frac{1}{2} \sum_{n=1, n\neq k}^{3} \frac{M_{nS}}{M_{kS}} i_{in,n}\right)} \quad (9)$$

The ration M_{nS}/M_{kS} can be obtained by equation (7), and the current $i_{in,n}$ and U_O are dc quantity that could be directly monitored.

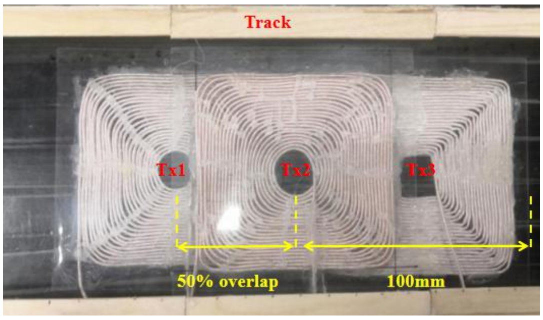

(a) Tx array

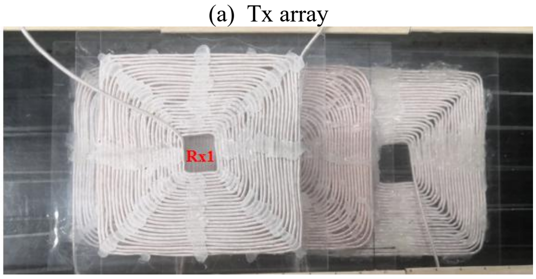

(b) Rx and Txs

Fig.3:Experiment Platform

2.4 Optimized voltage input based on load impedance

The reflected load of secondary sides is shifting unceasingly due to the vehicles motion. Therefore, the optimized impedance of the load is not constant. According to the maximum total efficiency, the optimum load resistance could be written as

$$R_{L,opt} = R_S \sqrt{1 + \frac{\omega^2 \sum_{n=1}^{3} M_{nS}^2}{R_P R_S}} \tag{10}$$

From the voltage conversion of the full-bridge diode converter, the optimum output voltage is

$$U_{O,opt} = \sqrt{R_{L,opt} U_O I_O} \tag{11}$$

The ac current goes through the Tx could be expressed as

$$i_{P,k,opt} = \frac{4}{\pi^2} \frac{M_{kS}\left(\frac{R_S}{R_{L,opt}} + 1\right)}{\omega \sum_{n=1}^{3} M_{nS}^2} \sqrt{R_{L,opt} U_O I_O}\,) \tag{12}$$

The optimum input voltage is the multiplication of equivalent $i_{p,k,opt}$ and input resistance $R_{in,k}$.

$$U_{in,k,opt} = \frac{\pi^2}{4} i_{P,k,opt} \left(\frac{\omega^2 \sum_{n=1}^{3} M_n^2}{R_S + R_{L,opt}} + R_P \right) \tag{13}$$

2.5 Control scheme and indications

From the previous derivation of the optimum voltage, the real-time primary inputs and load outputs should be continuously monitored during the time. The control logic and the cycle loop is demonstrated in Fig. 2. After sensing the feedback of U_{in} and i_{in}, the ratio of mutual inductance can be

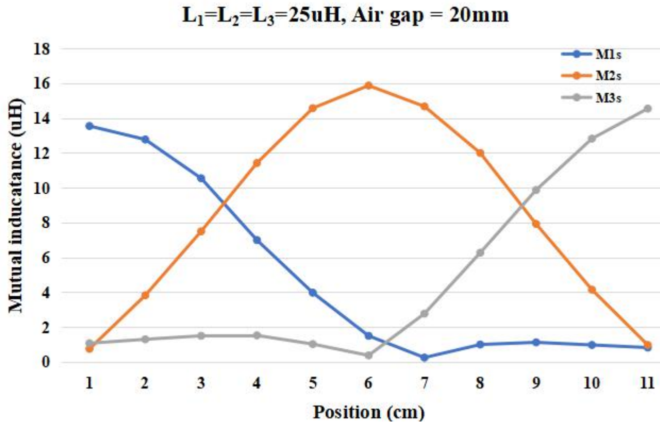

Fig.4: Mutual inductance between Txs and Rx with motion position

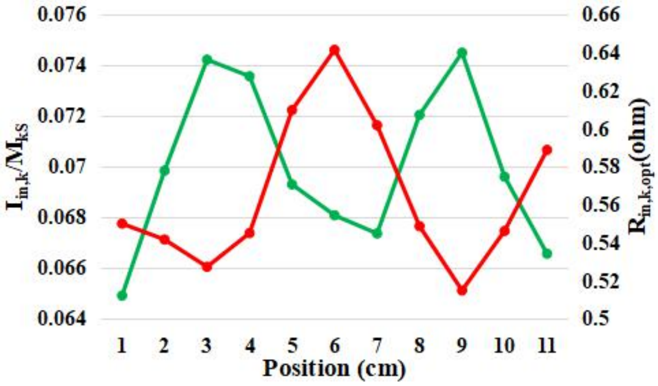

Fig.5: The proportional factor $i_{in,k}/M_{kS}$ and the optimum load impedance

calculated by using equation (7). And the exact mutual inductance is yielded in equation (9). The optimum input voltage $U_{in,k,opt}$ for each Tx is obtained by integrating the expected load impedance.

III. Simulation and Experiment Results

3.1 Experiment setup

The Tx and Rx are both designed as the same size of 100mm*100mm, 25 turns. Hence, they share the similar inductance as 25μH. The prototype is also reduced to a smaller scale proportionally, where the air gap is set to be 20mm. The switching frequency of the inverter is 20kHz, and this is also inherited for the design of the resonant circuit. To neutralizing higher order harmonic distortion when the Rx is fully alignment to one Tx, the compensated capacitance is chosen as 5.6μF. The copper wire resistance in the inductance are measured to be 0.3Ω for each coil. The key parameters of the setup are listed in Table I.

The three Txs are placed as 50% overlapped to each other, as demonstrated in Fig. 3. The Rx is regulated by a wooden track where only horizontal movement are allowed. It simulated the driving manner of a EV without vertical vibration.

3.2 Experiment results

The horizontal range is 200mm, so the measurement of mutual inductance are divided into 11 sampling points (in 10mm interval). The mutual inductance between each Tx and Rx are shown in Fig. 3. After integrating the results into PSIM simulation , the proportional factor $i_{in,k}/M_{kS}$ can be subsequently calculated, and the optimized load resistance are also derived. As can be seen in Fig. 4, the aforementioned factor is reverse proportional to the optimized resistance. It means that the power input of the Tx should be adjusted to a lower level when its coupling with Rx is weak. The controlled

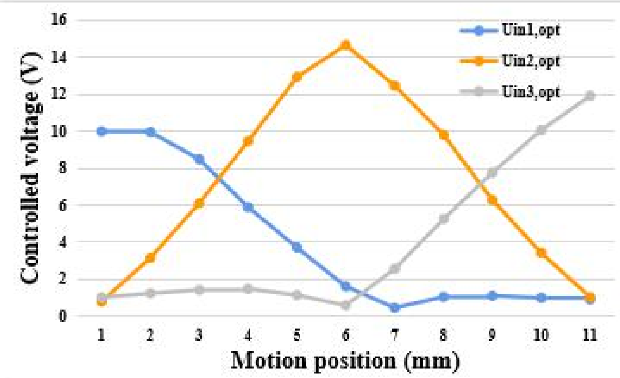

Fig.6: Voltage for each Tx after control

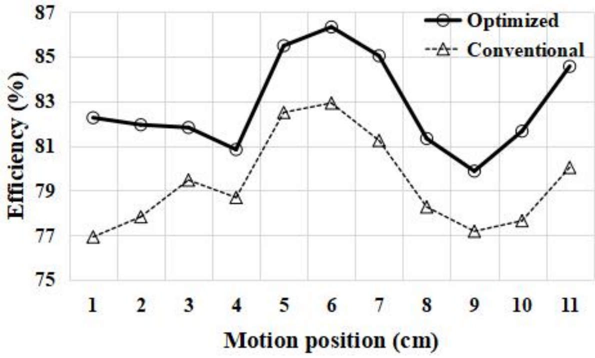

Fig.7: Total efficiency with optimized voltage inputs

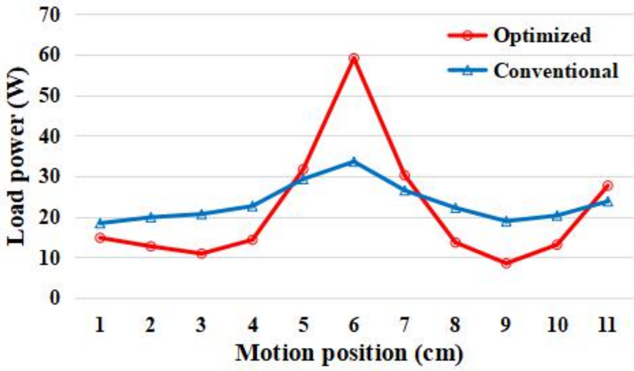

Fig.8: Load power after optimization

voltage for Tx windings are depicted in Fig. 6.

The total efficiency in each sampling points before and after optimization is shown in Fig. 7. The waveform in dash line is the efficiency by applying the same voltage input to Txs, and the waveform in solid line is the one of adopting the proposed control scheme. The trend of the total efficiency follows the variation of mutual inductance. As can be concluded in Fig. 7, the total efficiency is improved universally in all movement range, and the raise can be up to 5.2% when the coupling is stronger.

3.3 Discussions

For a series-series LC resonant compensation, the compensation capacitance is unchangeable once the design process is finished. Despite of the capacitor is compensated the leakage when the Tx and Rx are fully aligned, the leakage inductance is still altered badly due to the movement of Rx. Hence, when the coupling is stronger, the influence brought by the mis-designed compensation is reduced and the power output could be higher than the conventional system. As drawn in Fig. 8, the coupling between Rx and Tx array is highest in point 6, and the power output has its peak in this point. But when the coupling becomes weak, the efficiency also drops rapidly. And with the control algorithm, the input voltage for one specific Tx stays at a lower level when this Tx is misalignment, so the power output is lower than the conventional system.

Therefore, this discussed explanation indicates the necessity to link a dc/dc buck-boost converter, rather than directly output the power to load. By adjusting the duty cycle of the converter, the voltage output can be controlled stably. For a dc linear load, the equivalent load impedance can be still easily calculated due to its clear relation with duty cycle. The configuration of the system can be seen in many other researches[9-12].

IV. CONCLUSION

A control scheme that is aimed at achieving maximum total efficiency of EV dynamic charging is proposed in this paper. The relation of coupling and circuit dc outputs are found, and the outputs are real-time monitored for calculating the Tx input voltage. By adopting this method to simple LC compensated charging charging prototype(a 3*100mm*100mm Tx array, a 100mm*100mm receiver), the power efficiency is proved to be improved up to 5.2% in experiment. However, the LC compensation is sensitive to the misalignment that causes low robustness in power output. The method to obtain a robust power for linear load is discussed.

ACKNOWLEDGMENTS

This work is supported by the National Science Foundation of China under Grant U1913214.

REFERENCES

[1] Cui, Shumei, Wang, Zhiyuan, Han, Shouliang, Zhu, Chunbo, & Chan, C. C. (2019). Analysis and Design of Multiphase Receiver With Reduction of Output Fluctuation for EV Dynamic Wireless Charging System. IEEE Transactions on Power Electronics, 34(5), 4112-4124.

[2] Jeong, Seog Y, Park, Jun H, Hong, Gwang P, & Rim, Chun T. (2019). Autotuning Control System by Variation of Self-Inductance for Dynamic Wireless EV Charging With Small Air Gap. IEEE Transactions on Power Electronics, 34(6), 5165-5174.

[3] Huh, Sungryul, & Ahn, Dukju. (2018). Two-Transmitter Wireless Power Transfer with Optimal Activation and Current Selection of Transmitters. IEEE Transactions on Power Electronics, 33(6), 4957-4967.

[4] Zhong, W. X, & Hui, S. Y. R. (2015). Maximum Energy Efficiency Tracking for Wireless Power Transfer Systems. IEEE Transactions on Power Electronics, 30(7), 4025-4034.

[5] Minfan Fu, He Yin, Xinen Zhu, & Chengbin Ma. (2015). Analysis and Tracking of Optimal Load in Wireless Power Transfer Systems. IEEE Transactions on Power Electronics, 30(7), 3952-3963.

[6] Yeo, Tae-Dong, Kwon, DukSoo, Khang, Seung-Tae, & Yu, Jong-Won. (2017). Design of Maximum Efficiency Tracking Control Scheme for Closed-Loop Wireless Power Charging System Employing Series Resonant Tank. IEEE Transactions on Power Electronics, 32(1), 471-478.

[7] Huang, Zhicong, Wong, Siu-Chung, & Tse, Chi K. (2018). Control Design for Optimizing Efficiency in Inductive Power Transfer Systems. IEEE Transactions on Power Electronics, 33(5), 4523-4534.

[8] Kim, Do-Hyeon, Kim, Seongmin, Kim, Sang-Won, Moon, Jungick, Cho, Inkui, & Ahn, Dukju. (2020). Coupling Extraction and Maximum Efficiency Tracking for Multiple Concurrent Transmitters in Dynamic Wireless Charging. IEEE Transactions on Power Electronics, 35(8), 7853-7862.

[9] Jiwariyavej, Vissuta, Imura, Takehiro, & Hori, Yoichi. (2015). Coupling Coefficients Estimation of Wireless Power Transfer System via Magnetic Resonance Coupling Using Information From Either

Side of the System. IEEE Journal of Emerging and Selected Topics in Power Electronics, 3(1), 191-200.
[10] Kobayashi, Daita, Imura, Takehiro, & Hori, Yoichi. (2015). Real-time coupling coefficient estimation and maximum efficiency control on dynamic wireless power transfer for electric vehicles. 2015 IEEE PELS Workshop on Emerging Technologies: Wireless Power (2015 WoW), 1-6.
[11] Dai, Xin, Li, Xiaofei, Li, Yanling, & Hu, Aiguo Patrick. (2018). Maximum Efficiency Tracking for Wireless Power Transfer Systems With Dynamic Coupling Coefficient Estimation. IEEE Transactions on Power Electronics, 33(6), 5005-5015.
[12] Li, Hongchang, Li, Jie, Wang, Kangping, Chen, Wenjie, & Yang, Xu. (2015). A Maximum Efficiency Point Tracking Control Scheme for Wireless Power Transfer Systems Using Magnetic Resonant Coupling. IEEE Transactions on Power Electronics, 30(7), 3998-4008.